



Article

# The Effects of Air-Entraining Agent on Fresh and Hardened Properties of 3D Concrete

Ella Spurina <sup>1,\*</sup>, Maris Sinka <sup>1</sup>, Kristis Ziemelis <sup>1</sup>, Andris Vanags <sup>2</sup> and Diana Bajare <sup>3,\*</sup>

<sup>1</sup> 3D Concrete Printing Laboratory, Institute of Materials and Structures, Riga Technical University, 1 Paula Valdena Street, 1048 Riga, Latvia

<sup>2</sup> JSC Sakret Holdings, Ropazu nov., Stopinu pag., Rumbula, 2121 Riga, Latvia

<sup>3</sup> Institute of Materials and Structures, Riga Technical University, 6B Kipsalas Street, 1048 Riga, Latvia

\* Correspondence: ella.spurina\_1@rtu.lv (E.S.); diana.bajare@rtu.lv (D.B.)

**Abstract:** Three-dimensional concrete printing (3DCP) is becoming more common in the construction industry nowadays; however, the aspect of durability of printed concrete is not well-studied yet. Frost resistance is a very important factor for durability of concrete structures located in northern regions. Since air-entraining agents (AEAs) are widely used in conventional concrete, this paper focuses on exploring the potential of using AEAs in 3D concrete as well—the main objective is to determine how it affects fresh and hardened properties, including frost resistance of 3D concrete. Three different mixes were printed and cast—the dry mix consisted of ordinary Portland cement (OPC), limestone filler (LF), sand, as well as viscosity modifying agent (VMA) and superplasticizer (SP). Two mixes contained different amounts of AEA, the third one was used as reference. First, fresh state properties were tested—air content, density, and mini cone flow test. Second, 28-day compressive and flexural strength tests were carried out; bulk and particle densities were also determined. Next, both cast and printed concrete samples were subject to freeze–thaw cycles according to provisions of CEN/TS 12390-9, mass loss due to surface scaling was determined for each sample. As a result, printed concrete samples containing AEA in the amount of 0.06% of binder mass showed the highest frost resistance—addition of AEA decreased both flexural and compressive strength of this printed concrete mix by 30–40%. To conclude, the obtained results give an insight of how addition of AEA to printed concrete mix affects its properties both in long and short term. Further research of certain aspects, for instance, the air void system and pore distribution is needed to gain a deeper understanding on how to increase durability of 3D concrete.

**Keywords:** 3DCP; AEA; limestone filler; flexural strength; compressive strength; freeze–thaw



**Citation:** Spurina, E.; Sinka, M.; Ziemelis, K.; Vanags, A.; Bajare, D. The Effects of Air-Entraining Agent on Fresh and Hardened Properties of 3D Concrete. *J. Compos. Sci.* **2022**, *6*, 281. <https://doi.org/10.3390/jcs6100281>

Academic Editors: Yan Zhuge, Zhenhua Duan and Wahid Ferdous

Received: 8 August 2022

Accepted: 23 September 2022

Published: 26 September 2022

**Publisher's Note:** MDPI stays neutral with regard to jurisdictional claims in published maps and institutional affiliations.



**Copyright:** © 2022 by the authors. Licensee MDPI, Basel, Switzerland. This article is an open access article distributed under the terms and conditions of the Creative Commons Attribution (CC BY) license (<https://creativecommons.org/licenses/by/4.0/>).

## 1. Introduction

Three-dimensional printed concrete (3DPC) is a relatively new method used in the construction process worldwide in the latest few years. The increasing labor cost is one of the main drives for developing new 3D printing technologies for concrete as it allows for both time and money to be saved by introducing a certain degree of automation during the construction process. The automated process of 3D printing also allows for waste to be significantly reduced in the form of leftover concrete during construction by using topology optimization. In addition, 3DPC has lower constraints for geometrical freedom of structures, thus allowing for the creation of new and innovative architectural solutions by printing concrete in shapes that are more challenging when conventional cast concrete is used [1–3].

There are still many issues that are not fully resolved in the process of concrete 3D printing, for instance, durability of the printed concrete. Frost resistance is a vital factor in cooler climates as concrete structures, especially 3D printed ones, are exposed to freeze–thaw cycles as well as moisture which have a negative long-term effect on the

properties and surface quality of concrete structures. When water expands due to freezing, the material suffers from internal micro-cracking, causing progressive scaling of surfaces until complete concrete deterioration [4].

AEAs (air-entraining agents) are complex surfactant mixtures that are utilized to improve the frost durability of concrete [5]. The AEA adsorbs onto the cement particles to enhance particle surface activity and promote particle adsorption at the bubble air/water interface. If the air bubbles persist to become an adequate air void system in the hardened concrete, the air voids will provide protection against both internal frost damage and salt scaling, providing the air voids remain sufficiently empty. In the absence of AEAs, the air volume in concrete is typically within the range of ~1–3%, composed primarily of voids greater than 0.5 mm [5].

ACI 201.2R [6] recommends that air content for frost-resistant concrete mortar prepared without coarse aggregates be 9% if exposed to severe weather conditions and 7% if exposed to moderate conditions. EN 206-1 [7] states that the optimum air content is 5–6% in concrete containing no coarse aggregates [2].

Use of AEAs can alter rheological as well as hardened state properties of 3D concrete—improve workability, reduce exudation tendency, and decrease the drying shrinkage [8]. Rheology is a very important factor in 3D concrete as it affects several other aspects of 3D printing, such as extrudability, buildability, pumpability, and overall printability of the material; therefore, it is vital to evaluate both fresh and hardened properties of the 3D concrete mixes.

There are several papers published on the use of AEA in both conventional and 3D concrete, for instance, research carried out by Zhang et al. [9] concluded that ordinary concrete samples with  $w/c = 0.53$  show no significant reduction in compressive strength if 4–5% air is used, but above 7% it causes a sharp decline in compressive strength. Tarhan and Sahin [10] carried out research on fresh state behavior as well as compressive strength of air-entrained 3D concrete—they found that the addition of AEA dramatically decreased compressive strength of 3D concrete, as well as its viscosity and shear stress. Das et al. [11] concluded that the extrusion and pumping process involved in concrete 3D printing could worsen frost resistance of air-entrained concrete by destabilizing its air void structure.

Many authors [12–17] have conducted frost resistance tests based on the methodology prescribed by CEN/TS 12390-9 [18], ASTM C666 [19], or other relevant standards—measurement of mass loss due to scaling, changes in compressive strength, and dynamic modulus of elasticity of cast concrete. There is a limited amount of studies that focus on testing frost resistance of 3D printed concrete samples, for instance, Sikora et al. [16] based their test procedure on provisions of ASTM C666, used concrete samples with a size of  $40 \times 40 \times 160 \text{ mm}^3$  and determined weight and strength changes of each sample after a certain amount of freeze–thaw cycles, whereas, Assaad et al. [2] tested printed layer bond strength and cumulative mass loss after subjecting the samples to a certain amount of freeze–thaw cycles according to provisions of CEN/TS 12390-9 as part of their research. Weight loss of 3D printed specimens was found to be lower than that of mold cast specimens indicating of a higher frost resistance in several studies [2,20]; however, Das et al. [16] found that after subjecting cast and 3D concrete to 300 freeze–thaw cycles according to provisions of ASTM C666, printed concrete had lower resistance to freeze–thaw conditions compared to their cast counterparts. In addition, Sikora et al. [16] found that the performance of 3D printed concrete under freezing and thawing cycles was very similar to cast concrete and showed high stability. Van der Puten et al. [21] came to similar conclusions—frost resistance of printed and cast samples was tested according to provisions of Belgian standard NBN B 15—231 [22] and no significant difference was determined between traditionally cast and printed samples. As the abovementioned previous research provides very contradicting results, it is vital to evaluate the freeze–thaw test method for printed samples and the main factors that might cause such contradicting results.

The main issue this paper focuses on is how different amounts of added AEA impacts both fresh and hardened properties of 3D printed concrete while using cast concrete samples of the same mixes for reference. All mixes are evaluated in terms of how suited they are

for 3D printing with the specific printer setup and settings, as well as how addition of AEA affects frost resistance and compressive and flexural strength of printed concrete samples—all of these properties are related to increases in durability of the printed concrete, which can lead 3D concrete to become more widely used in the construction industry.

## 2. Materials and Methods

### 2.1. Concrete Mixes

The experimental dry mixture consisted of OPC CEM I 42.N by SCHWENK Ltd. (Brocēni, Latvia), limestone filler by Saulkalne S Ltd. (Salaspils, Latvia)—a powder material with a fineness of less than 1 mm (99.9%), sand by SAKRET Ltd. (Latvia) with particle size ranging from 0 to 2 mm, density of 1.5–1.6 g/cm<sup>3</sup>, fineness category F3—all obtained from local plants in Latvia, as well as powder-type viscosity modifying agent (VMA) by Se Tylose GmbH & Co (Wiesbaden, Germany)—sodium carboxymethyl cellulose (Na-CMC). Amount of the added VMA was 0.2% of total dry mixture mass. Commercial high-range water reducing agent (HRWRA) Dynamon SP-1 by MAPEI Ltd. (Italy) was used to obtain the necessary rheological properties for the concrete mix. The amount of added HRWRA was 0.45% of total binder mass. SikaAIR by SIKA AG (Switzerland) which is based on synthetic surfactants was used as air entraining agent.

Three different concrete mixes were used for 3D printing, casting, and testing—the first one (mix AEA-000) contained limestone filler as well as additives for enhancing rheological properties of the mixture and was used as a reference whereas the other two mixes had different amounts (0.06% and 0.12% of binder mass) of AEA added to the dry mass together with water—Mix AEA-006 and Mix AEA-012 accordingly. The ingredients for all mixes were proportioned by mass. The experimental mixture proportioning of concrete was obtained through previous research ensuring that it has the necessary extrudability and buildability for carrying out the further tests. See Table 1 for all mix proportions of the concrete used for 3D printing, casting, and testing.

**Table 1.** Concrete mix proportions for Mix AEA-000, Mix AEA-006, and AEA-012 (amounts expressed in grams per 1000 g of dry mixture).

Mix	Water	OPC	Sand 0–2 mm	Limestone Filler	SP *	VMA *	AEA *	W/OPC *
AEA-000	155	328	564	108	1.5	0.2	-	0.47
AEA-006	155	328	564	108	1.5	0.2	0.197	0.47
AEA-012	155	328	564	108	1.5	0.2	0.394	0.47

\* Note: SP = superplasticizer, VMA = viscosity modifying agent, AEA = air-entraining agent, OPC = ordinary Portland cement, W = water.

### 2.2. Mixing, 3D Printing and Curing

The inside room temperature was 19–21 °C, relative air humidity between 20–30% throughout the whole mixing, printing, and curing process. Mixing was carried out using a portable mortar mixer RUBIMIX –9 N by RUBI UK LTD. (Rainham, United Kingdom) with a speed of 780 RPM. First, all dry ingredients were mixed for 60 s until the dry mass was homogenous. Second, tap water (t = 9–10 °C) mixed with HRWRA in the amount of 0.46% of binder mass was added to half of the dry mixture and mixed for 30 s, then the remaining dry mixture was gradually added and mixed for 30 s—this was carried out to facilitate the mixing process and ensure full hydration of the binder. Third, AEA and an additional 50 g of water was added to the mixture (except Mix AEA-000) and mixed for another 60 s. Next, fresh state properties of mortar were tested—see Section 2.3 for a description of tests.

Three-dimensional printing was performed with a custom-made gantry type printer developed within RTU for the printing of concrete and other building materials. The printer has a 2000 × 1000 × 1200 (h) mm aluminum frame allowing for maximum model dimensions of 1260 × 417 × 844, max load capacity of hopper—300 kg. Repetier-Host by GmbH & Co. KG. (Willich, Germany) and customized open source Repetier-Firmware were

used for controlling the printer, slicing was carried out using Simplify3D by Simplify3D Ltd. (Cincinnati, OH, United States). Printhead nozzle diameter—25 mm, layer width—40 mm, layer height—10 mm. Printer configuration is shown in Figure 1.

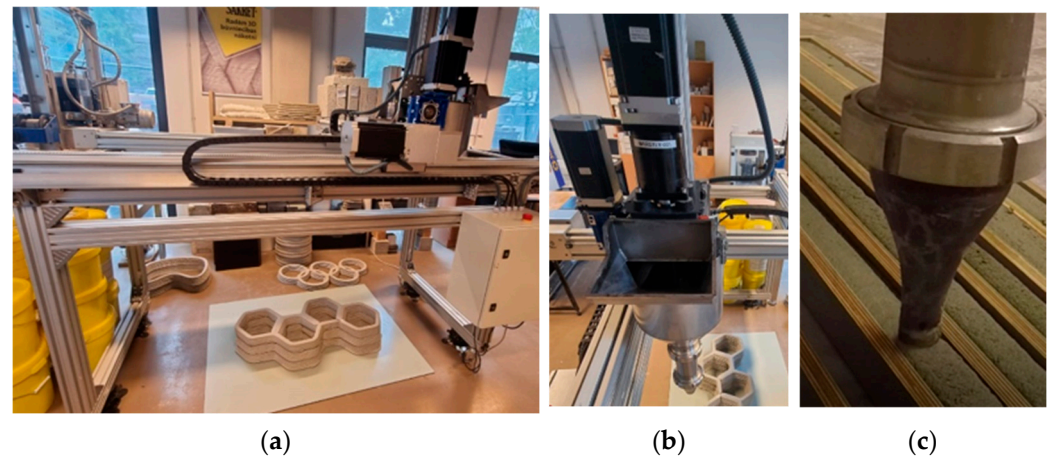


**Figure 1.** Three-dimensional printer (a), printer hopper (b), and nozzle (c).

The mixed concrete was filled into the hopper and extruded through the printhead until a homogenous mass of concrete was flowing through the nozzle. After that, each concrete mixture was printed into pre-prepared molds resembling modified molds for casting concrete samples used in flexural strength tests—height and width of 40 mm and length of 960 mm, printing speed of 800 mm/min. Molds were used to avoid voids caused by layering and to ensure a smooth surface for testing—see Figure 2b. After curing, each molded line was sawed into 6 samples with a length of 160 mm each. The layer height of 10 mm remained the same throughout the printing process—4 layers were printed into the molds creating a model with total height of 40 mm. A total of 12 samples were printed using each concrete mix—see the printed models in Figure 2.

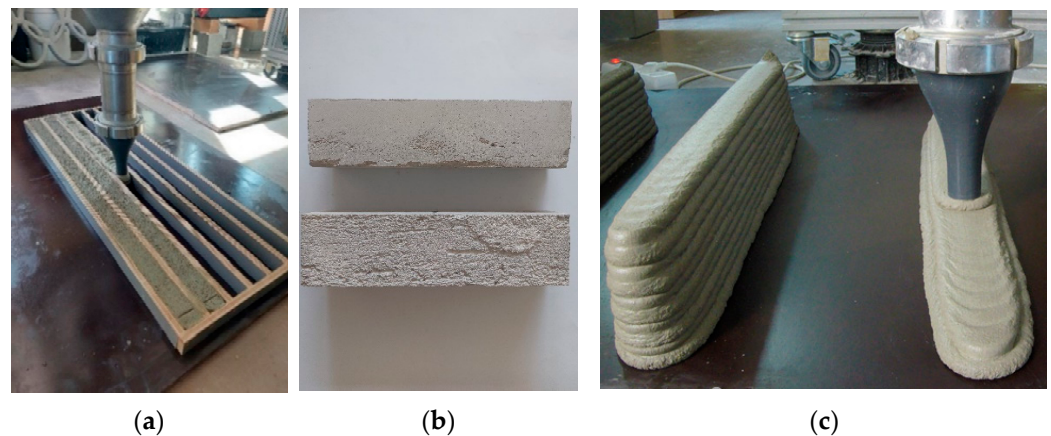


**Figure 2.** Printed models in molds for mechanical strength tests (a), demolded printed models for mechanical strength tests (top—side surface; bottom—top surface (b), and frost resistance tests (c).

Next, the samples for frost resistance tests were printed—500 mm long straight lines consisting of 10 layers—each 10 mm high and  $50 \pm 5$  mm wide, printing speed of 1200 mm/min, which were divided into 100 mm wide samples whilst still in fresh state 40–60 min after printing.

The reference samples were cast at the same time as 3D printing was carried out—the mortar was filled into the molds without extruding it through the printhead. Molding of test samples was carried out according to provisions of EN 12390-2 [23] and EN 196-1 [24]—4 cubes were cast and later on sawed in half for freeze–thaw testing, in addition, 6 samples sized  $40 \times 40 \times 160$  mm were cast for strength tests.

Both cast and printed samples were cured at room temperature (19–21 °C), relative humidity between 20–35% as providing high moisture conditions for printed models was not possible due to their size; all samples were covered with a PE sheet for the first 48 h, cast samples were demolded after 48 h and stored next to printed samples.

### 2.3. Testing

#### 2.3.1. Fresh State Properties

First, a mini cone slump test according to EN 1015-3 [25] was carried out once for each of the fresh mortars by jolting the table 15 and 25 times, also—vertical slump was determined right before loading the mortars into the printer hopper—see Figure 3a. Second, fresh mortar density as well as air content was measured once for each mix according to the provisions of EN 12350-7 [26] by using an 8L air entrainment meter with hand pump—see Figure 3b,c. Next, extrudability and buildability tests were carried out once for each mix before printing the actual models. After printing, a 50 mm wide line it was visually examined and evaluated for cracks and inhomogeneity—lack of which allowed the concrete mix to pass the extrudability test as in a properly extruded process there should be no discontinuity in the layers and no gaps in the extruded mixtures [27,28]. Previous research has also used similar approach of visually inspecting a predetermined printed model in order to evaluate its extrudability [28–30]. As there were no other specific requirements for these concrete mixes regarding buildability, the buildability test consisted of printing a model of a 10-layer high 500 mm long line—corresponding to the size of test samples—without its collapse. Similar approach has been used and described in other previous research [28,31].

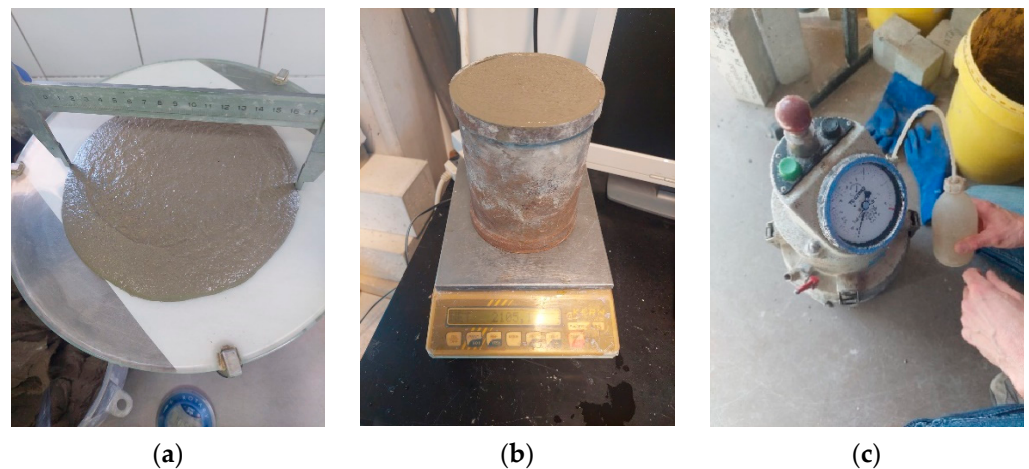


**Figure 3.** Fresh state property testing: mini cone slump (a), density (b), and air content (c).

#### 2.3.2. Density, Flexural, and Compressive Strength

First, all samples were weighed and measured to determine material density; one of each sample was ground by using a laboratory grinder mill—the obtained powder was used to determine particle density by using the Le Chatelier flask. Next, flexural, and compressive strength tests were carried out in accordance with standard EN 1015-11 [32]. For the printed samples, both flexural and compressive strength was tested for 3 samples of each series parallel to printing direction. Testing was carried out by using a testing machine, “Controls 50-C56Z00” by Controls S.p.A. (Italy); testing speed was set to 1.0 MPa/s for compressive strength, 0.5 mm/s for flexural strength.

#### 2.3.3. Frost Resistance

Frost resistance was tested by exposing the samples to freeze–thaw cycles according to the provisions of CEN 12390-9—modified slab tests were carried out by submerging the test surfaces in 3% NaCl solution and placing them in a climatic test chamber. The

freeze–thaw resistance was evaluated by the measurement of mass scaled from concrete sample surface area after 14, 28 and 56 freeze–thaw cycles.

As mentioned in Section 2.2, printed samples for frost resistance testing were obtained by sawing the edges of a printed straight line, whereas cast samples were obtained by sawing cubic samples with an edge length of 100 mm in half. Three samples of each kind were tested. After a certain number of cycles, the mass loss was determined for each sample with precision of 0.1 g. The results were expressed in g/m<sup>2</sup> of exposed surface area—for printed samples the projected area was measured without considering the grooves formed by layers.

### 3. Results and Discussion

#### 3.1. Fresh State Properties

Results from all fresh state property tests are summarized in Table 2 below. Mix AEA-000 contained 8.5% of air which is a relatively high amount for a mix containing no AEA—this can be explained by the presence of sodium carboxymethyl cellulose (used as VMA) in the concrete mix. The fact that the use of cellulose based VMAs increases the amount of entrained coarse air voids and with it, porosity, causing decreased mechanical properties of concrete has been described in previous research [33,34]. The addition of 0.06% of AEA increased the air amount in the concrete mix AEA-006 to 14.0%—the amount of entrained air increased by 65% compared to the mix without any AEA. Air content in mix AEA-012, however, was 15%, which is a 76% increase when compared to mix AEA-000. The air content values exceed the minimum air content value of 6.0–11.5% for frost resistant concrete (exposure classes XF1–XF4) determined by annex BS 8500-1 [35] to EN 206-1, indicating that the strength reduction by additional entrained air is unnecessary as it possibly adds little value in enhancing frost resistance. Interaction of the AEA with other additives used in this specific concrete mix should be evaluated as it is very likely that VMA has entrained too many coarse air voids into the mix. Fresh state density of Mix AEA-000 was 2105 kg/m<sup>3</sup>, it was decreased by 68% to 1962 kg/m<sup>3</sup> for mix AEA-006 and by 79% to 1938 kg/m<sup>3</sup> for mix AEA-012—these values roughly correspond to the amounts measured of entrained air in the mixes, indicating the level of precision of the used method for measuring it.

**Table 2.** Fresh state properties of mixes AEA-00, AEA-006, and AEA-012.

Mix	Measured Air Content, %	Fresh State Density, kg/m <sup>3</sup>	Slump Ø × 15, mm	Slump Ø × 25, mm	Vertical Slump, mm
AEA-000	8.5	2105	171	180	10
AEA-006	14.0	1962	156	172	4
AEA-012	15.0	1938	150	169	3

Mix AEA-000 which contained no air-entraining additive, had the highest slump diameter values of 171 mm and 180 mm after 15 and 25 jolts accordingly, and a vertical slump value of 10 mm. Addition of 0.06% of AEA decreased horizontal values to 156 and 172 mm accordingly, as well as vertical slump value to 4 mm. Concrete mix containing 0.12% AEA had the highest rate of plastic viscosity with slump diameters of 150 and 169 mm, and vertical slump of 3 mm. This coincides with previous research [6,36] indicating that the entrained air bubbles increase the yield stress point of mortar which contributes to geometrical stability of 3D printed concrete layers. Although, all mixes passed the extrudability and buildability of the pre-tests before the actual models were printed, it was obvious that the addition of AEA to the 3D concrete mix had a positive impact on overall printability of concrete as the air-entrained mass could still be extruded from the nozzle without any visual defects of the layers, but had a much better buildability than the non- air-entrained mix as the slump value was lower (especially the vertical slump); therefore, the printed layers of air-entrained mixes could sustain their initial form better than the printed non-entrained mix. This coincides with the previous research [37,38].

It must be noted that the workability and viscosity of the mix containing 0.12% of AEA (maximum recommended percentage of AEA advised by manufacturer is 0.15%) did not differ significantly from the mix with AEA-006, which contained half the amount of AEA, indicating a dosage level after which the properties of concrete mix are not altered even with the addition of a significantly high amount of AEA to it. Ouyung et al. [39] also found a plateau for the increment of air content and workability of concrete forms after adding a certain value of AEA to the mix.

### 3.2. Hardened Properties

As depicted in Table 3, bulk density of cast samples was slightly higher than that of the printed ones; for mixes AEA-000 and AEA-006, the difference was within the limits of standard deviation; however, printed samples of the AEA-012 mix had a 4% lower bulk density than cast samples of the same mix. Particle density of the dry mix was 2615 kg/m<sup>3</sup>, which allowed the calculation of the void ratio for each series of samples—see Equation (1).

$$P_k = \left( 1 - \frac{\rho_0}{\rho} \right) \cdot 100\% , \tag{1}$$

where P<sub>k</sub>—void ratio; ρ<sub>0</sub>—bulk density of sample; ρ—particle density of sample.

**Table 3.** Density of printed and cast samples of mixes AEA-00, AEA-006, and AEA-012.

Cast Mix	Printed Mix	Bulk Density, kg/m <sup>3</sup>	Particle Density, kg/m <sup>3</sup>	Void Ratio, %
AEA-000		2044 ± 33		21
	AEA-000	2011 ± 62		23
AEA-006		1769 ± 74	2615 ± 82	32
	AEA-006	1746 ± 26		33
AEA-012		1752 ± 32		33
	AEA-012	1689 ± 20		35

Void ratios for printed and cast samples of the same mix did not differ significantly, indicating that the concrete mass of printed samples was not layered and did not contain any major voids due to the selected printing method in molds.

Printed samples of mix containing 0.12% of AEA and 15.0% entrained air had the lowest density, 1689 ± 20 kg/m<sup>3</sup>, whereas samples printed of a mix with 0.06% of AEA and 14.0% entrained air had density of 1746 ± 26 kg/m<sup>3</sup>, which is a 16% and 13% decrease compared to the density of the printed mix without air-entraining additives (2011 ± 62 kg/m<sup>3</sup>).

Figure 4a shows that mean 28-day flexural strength of printed samples, as expected, was lower than that of cast ones for all mixes; however, the biggest difference was for mix AEA-006—mean flexural strength of printed samples of this mix was 1.8 MPa (25%) lower than that of cast samples. The addition of 0.06% of AEA to the concrete mix caused a decrease in flexural strength by 32% for printed samples (from 7.9 to 5.4 MPa), and by 14% for cast samples (8.3 to 7.1 MPa). Addition of 0.12% of AEA decreased flexural strength by 37% for printed samples (from 7.9 to 5.0 MPa), and by 32% for cast samples (8.3 to 5.7 MPa).

As per Figure 4b, the mean 28-day compressive strength of printed samples was also lower than that of cast ones for all mixes; AEA-000 showed the biggest difference—mean compressive strength of printed samples (30.8 MPa) of this mix was 9.3 MPa (23%) lower than that of cast samples (40.1 MPa). Addition of 0.06% of AEA to the concrete mix caused a decrease in compressive strength by 36% for printed samples (from 30.8 to 19.7 MPa), and by 33% for cast samples (40.1 to 26.7 MPa). Addition of 0.12% of AEA decreased compressive strength by 52% for printed samples (40.2 to 14.9 MPa), and by 45% for cast samples (40.2 to 22.0 MPa).

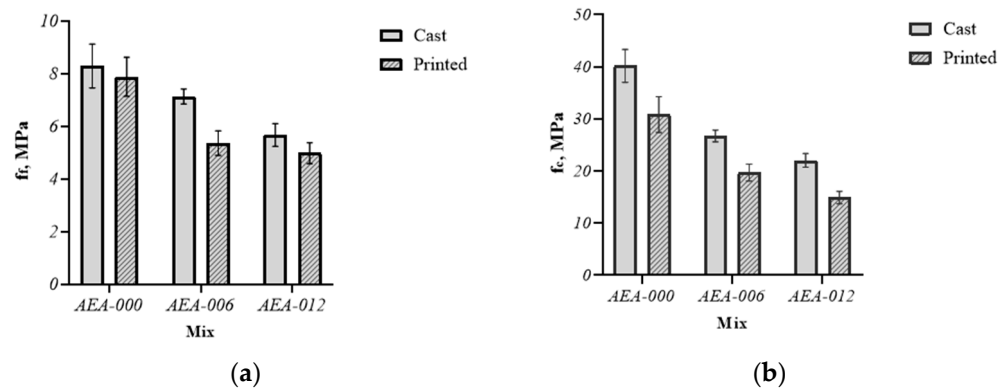


**Figure 4.** Flexural (a) and compressive (b) strength of 3D printed and cast samples.

Both mixes showed a decrease in both flexural and compressive strength, and density with the addition of air-entraining additive—strength reduction for samples containing AEA dosage of 0.06% and 0.12% of binder mass did not differ significantly, indicating a formation of a plateau after reaching the addition of AEA which does not alter the air content, as well as other fresh state and hardened properties of the concrete mix, which coincides with other published work on this matter [39]. As the time between layers was relatively low (~15 s) and the printed samples for strength tests were extruded into molds, it is considered that layer bonding does not affect mechanical properties of printed samples significantly; this was also confirmed by the visual inspection of samples before and after testing.

As depicted in Figure 5, 3D printed and cast samples of mix AEA-000 showed mass loss due to scaling in the amount of 406 and 87 g/m<sup>2</sup> accordingly after being subject to 56 freeze–thaw cycles. The addition of 0.06% of AEA achieved the highest frost resistance out of all mixes—it decreased mass loss of test samples 6.4 times for printed samples (63 g/m<sup>2</sup>), as well as 3.4 times for cast samples (25 g/m<sup>2</sup>). Printed and cast samples of mix AEA-012 had a mass loss in the amount of 83 and 37 g/m<sup>2</sup>, accordingly, after being subjected to 56 freeze–thaw cycles, which indicates a lower frost resistance with the addition of AEA in the amount of 0.12% of binder mass than for 0.06%.

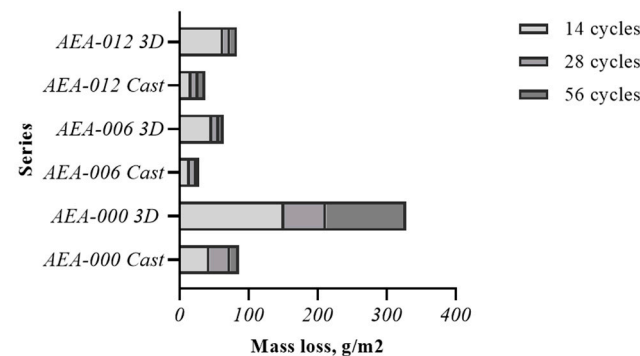


**Figure 5.** Mass loss of 3D printed and cast samples after freeze–thaw cycles.

As the obtained frost resistance test results of 3D printed concrete are in line with the provisions for concrete class XF4 according to Annex LVS 156-1 [40] to EN 206-1 (mass loss due to surface scaling after 56 freeze–thaw cycles less than 350 g/m<sup>2</sup>), the concrete mix might be suitable for use in 3D printed structures exposed to freezing conditions; however, further research has to be carried out regarding other aspects, such as sulfate and chloride resistance, air void distribution as well as use of other additives in order to increase its durability.

An increase in air content for the 3D concrete mix by use of AEA decreased its density and flexural and compressive strength, while improving its buildability and frost resistance.



An increased amount of entrained air could allow for decreased material consumption when printing a similar structure with non-air-entrained concrete, while increasing its frost resistance. Printed samples of the AEA-006 mix that showed the highest frost resistance, had a flexural strength of 5.4 MPa and compressive strength of 19.7 MPa, which indicates that the concrete mix might be used for single story buildings or other structures that do not need to withstand high loads. As the obtained frost resistance values are relatively high—corresponding to class XF4, the amount of entrained air could be reduced in order to minimize the decrease in strength of the printed concrete. Further research needs to be carried out in order to evaluate the appropriate amount of AEA, as well as the air void and pore structure of the concrete in order to find a balance between buildability, workability, frost resistance, and strength.

#### 4. Conclusions

Use of air-entraining agents in a 3D concrete mix was evaluated as part of this research. It was found that the addition of AEA in the amount of 0.06% of binder mass did not differ significantly from the mix containing 0.12% of AEA in terms of both fresh and hardened properties. Overall, the presence of AEA increased the yield stress point, buildability, and with it, overall printability of 3D concrete compared with the same mix containing no AEA.

Entrained air caused a decrease in density, as well as both flexural and compressive strength of the printed concrete, affecting printed concrete more than the conventionally cast samples.

Printed samples had a lower frost resistance than cast ones, which is in line with some of the previously published work; however, there is also some contradiction in previously published research. The addition of AEA in the amount of 0.06% of the binder mass significantly increased the frost resistance of the printed and cast concrete.

Further research of certain aspects, for instance, the air void system and pore distribution, is needed to gain a deeper understanding on how to increase durability of 3D concrete. The reduced density caused by entrained air might offer a reduction in material consumption as well as an increase in the frost resistance of concrete mixes used in the 3D printing of structures exposed to weather.

**Author Contributions:** Conceptualization, E.S., M.S., K.Z., A.V. and D.B.; methodology, E.S., M.S. and D.B.; software, E.S.; validation, E.S. and M.S.; formal analysis, E.S. and M.S.; investigation, E.S. and M.S.; resources, K.Z., A.V. and D.B.; data curation, E.S. and M.S.; writing—original draft preparation, E.S. and M.S.; writing—review and editing, E.S., M.S. and D.B.; visualization, E.S. and M.S.; supervision, A.V. and D.B.; project administration, M.S. and D.B.; funding acquisition, M.S., K.Z. and A.V. All authors have read and agreed to the published version of the manuscript.

**Funding:** Kristis Ziemelis was supported by Riga Technical University's Doctoral Grant program. Maris Sinka was supported by the European Regional Development Fund within the Activity 1.1.1.2 "Post-doctoral Research Aid" of the Specific Aid Objective 1.1.1 "To increase the research and innovative capacity of scientific institutions of Latvia and the ability to attract external financing, investing in human resources and infrastructure" of the Operational Programme "Growth and Employment" (No.1.1.1.2/VIAA/3/19/394).

**Conflicts of Interest:** The authors declare no conflict of interest.

#### References

1. Hossain, A.; Zhumabekova, A.; Paul, S.C.; Kim, J.R.A. Review of 3D Printing in Construction and its Impact on the Labor Market. *Sustainability* **2020**, *12*, 8492. [CrossRef]
2. Mohan, M.K.; Rahul, A.V.; De Schutter, G.; Van Tittelboom, K. Extrusion-based concrete 3D printing from a material perspective: A state-of-the-art review. *Cem. Concr. Compos.* **2021**, *115*, 103855. [CrossRef]
3. Wu, P.; Wang, J.; Wang, X. A critical review of the use of 3-D printing in the construction industry. *Autom. Constr.* **2016**, *68*, 21–31. [CrossRef]
4. Assaad, J.J.; Hamzeh, F.; Hamad, B. Qualitative assessment of interfacial bonding in 3D printing concrete exposed to frost attack. *Case Stud. Constr. Mater.* **2020**, *13*, e00357. [CrossRef]

5. Tunstall, L.E.; Ley, M.T.; Scherer, G.W. Air entraining admixtures: Mechanisms, evaluations, and interactions. *Cem. Concr. Res.* **2021**, *150*, 106557. [[CrossRef](#)]
6. ACI Committee 201. *201.2R-16 Guide to Durable Concrete*; ACI: Farmington Hills, MI, USA, 2016; p. 84.
7. *EN 206+A2:2001*; Concrete—Part 1: Specification, Performance, Production and Conformity. NSAI: Northwood, Ireland, 2001.
8. Souza, M.T.; Ferreira, I.M.; Guzi de Moraes, E.; Senff, L.; Novaes de Oliveira, A.P. 3D printed concrete for large-scale buildings: An overview of rheology, printing parameters, chemical admixtures, reinforcements, and economic and environmental prospects. *J. Build. Eng.* **2020**, *32*, 101833. [[CrossRef](#)]
9. Zhang, P.; Li, D.; Qiao, Y.; Zhang, S.; Sun, C.; Zhao, T. Effect of air entrainment on the mechanical properties, chloride migration, and microstructure of ordinary concrete and fly ash concrete. *J. Mater. Civ. Eng.* **2018**, *30*, 04018265. [[CrossRef](#)]
10. Tarhan, Y.; Şahin, R. Fresh and Rheological Performances of Air-Entrained 3D Printable Mortars. *Materials* **2021**, *14*, 2409. [[CrossRef](#)] [[PubMed](#)]
11. Das, A.; Song, Y.; Mantellato, S.; Wangler, T.; Lange, D.A.; Flatt, R.J. Effect of processing on the air void system of 3D printed concrete. *Cem. Concr. Res.* **2022**, *156*, 106789. [[CrossRef](#)]
12. Gyurkó, Z.; Szijártó, A.; Nemes, R. Increasing Freeze-thaw Resistance of Concrete by Additions of Powdered Cellular Concrete and Clay Bricks. *Procedia Eng.* **2017**, *193*, 11–18. [[CrossRef](#)]
13. Łażniewska-Piekarczyk, B. The frost resistance versus air voids parameters of high performance self compacting concrete modified by non-air-entrained admixtures. *Constr. Build. Mater.* **2013**, *48*, 1209–1220. [[CrossRef](#)]
14. Kalhori, M.; Ramezani-pour, A.A. Innovative air entraining and air content measurement methods for roller compacted concrete in pavement applications. *Constr. Build. Mater.* **2021**, *279*, 122495. [[CrossRef](#)]
15. Mayercsik, N.P.; Vandamme, M.; Kurtis, K.E. Assessing the efficiency of entrained air voids for freeze-thaw durability through modeling. *Cem. Concr. Res.* **2016**, *88*, 43–59. [[CrossRef](#)]
16. Sikora, P.; Techman, M.; Federowicz, K.; El-Khayatt, A.M.; Saudi, H.A.; Elrahman, M.A.; Hoffmann, M.; Stephan, D.; Chung, S.Y. Insight into the microstructural and durability characteristics of 3D printed concrete: Cast versus printed specimens. *Case Stud. Constr. Mater.* **2022**, *17*, e01320. [[CrossRef](#)]
17. Das, A.; Sanchez, A.M.A.; Wangler, T.; Flatt, R.J. Freeze-Thaw Performance of 3D Printed Concrete: Influence of Interfaces. In Proceedings of the Third RILEM International Conference on Concrete and Digital Fabrication, Leicester, UK, 25 June 2022; pp. 200–205. [[CrossRef](#)]
18. *CEN/TS 12390-9:2016*; Testing Hardened Concrete—Part 9: Freeze-Thaw Resistance with De-Icing Salts-Scaling. BSI: Englewood, CO, USA, 2016.
19. *ASTM C666/C666M-15*; Standard Test Method for Resistance of Concrete to Rapid Freezing and Thawing. ASTM: West Conshohocken, PA, USA, 2015.
20. Nodehi, M.; Aguayo, F.; Nodehi, S.E.; Gholampour, A.; Ozbakkaloglu, T.; Gencil, O. Durability properties of 3D printed concrete (3DPC). *Autom. Constr.* **2022**, *142*, 104479. [[CrossRef](#)]
21. Van Der Putten, J.; De Volder, M.; Van den Heede, P.; Deprez, M.; Cnudde, V.; De Schutter, G.; Van Tittelboom, K. Transport properties of 3D printed cementitious materials with prolonged time gap between successive layers. *Cem. Concr. Res.* **2022**, *155*, 106777. [[CrossRef](#)]
22. *NBN B 15-231:1987*; Concrete Testing—Resistance to Freezing. SAI Global: Sydney, NSW, Australia, 1987.
23. *EN 12390-2:2019*; Testing Hardened Concrete-Part 2: Making and Curing Specimens for Strength Tests. BSI: Englewood, CO, USA, 2019.
24. *EN 196-1:2016*; Methods of Testing Cement-Part 1: Determination of Strength. BSI: Englewood, CO, USA, 2016.
25. *EN 1015-3:1999*; Methods of Test for Mortar for Masonry-Part 3: Determination of Consistence of Fresh Mortar (by Flow Table). BSI: Englewood, CO, USA, 1999.
26. *EN 12350-7:2019*; Testing Fresh Concrete-Part 7: Air Content-Pressure Methods. BSI: Englewood, CO, USA, 2019.
27. Saruhan, V.; Keskinates, M.; Felekoğlu, B. A comprehensive review on fresh state rheological properties of extrusion mortars designed for 3D printing applications. *Constr. Build. Mater.* **2022**, *337*, 127629. [[CrossRef](#)]
28. Rahul, A.V.; Santhanam, M.; Meena, H.; Ghani, Z. 3D printable concrete: Mixture design and test methods. *Cem. Concr. Compos.* **2019**, *97*, 13–23. [[CrossRef](#)]
29. Le, T.T.; Austin, S.A.; Lim, S.; Buswell, R.A.; Gibb, A.G.F.; Thorpe, T. Mix design and fresh properties for high-performance printing concrete. *Mater. Struct.* **2012**, *45*, 1221–1232. [[CrossRef](#)]
30. Ma, G.; Li, Z.; Wang, L. Printable properties of cementitious material containing copper tailings for extrusion based 3D printing. *Constr. Build. Mater.* **2018**, *162*, 613–627. [[CrossRef](#)]
31. Chen, Y.; He, S.; Zhang, Y.; Wan, Z.; Çopuroğlu, O.; Schlangen, E. 3D printing of calcined clay-limestone-based cementitious materials. *Cem. Concr.* **2021**, *149*, 106553. [[CrossRef](#)]
32. *EN 1015-11:2019*; Methods of Test for Mortar for Masonry—Part 11: Determination of Flexural and Compressive Strength of Hardened Mortar. BSI: Englewood, CO, USA, 2019.
33. Wang, S.; Zhang, G.; Wang, Z.; Huang, T.; Wang, P. Evolutions in the properties and microstructure of cement mortars containing hydroxyethyl methyl cellulose after controlling the air content. *Cem. Concr. Compos.* **2022**, *129*, 104487. [[CrossRef](#)]
34. Wyrzykowski, M.; Kiesewetter, R.; Münch, B.; Baumann, R.; Lura, P. Pore structure of mortars with cellulose ether additions—Study of the air-void structure. *Cem. Concr. Compos.* **2015**, *62*, 117–124. [[CrossRef](#)]

35. *BS 8500-1:2015+A2:2019; Concrete*. Complementary British Standard to BS EN 206—Method of Specifying and Guidance for the Specifier. BSI: Englewood, CO, USA, 2019.
36. Marchon, D.; Kawashima, S.; Bessaies-Bey, H.; Mantellato, S.; Ng, S. Hydration and rheology control of concrete for digital fabrication: Potential admixtures and cement chemistry. *Cem. Concr. Res.* **2018**, *112*, 96–110. [[CrossRef](#)]
37. Tay, Y.W.D.; Qian, Y.; Tan, M.J. Printability region for 3D concrete printing using slump and slump flow test. *Compos. Part. B Eng.* **2019**, *174*, 106968. [[CrossRef](#)]
38. Jiang, Q.; Liu, Q.; Wu, S.; Zheng, H.; Sun, W. Modification effect of nanosilica and polypropylene fiber for extrusion-based 3D printing concrete: Printability and mechanical anisotropy. *Addit. Manuf.* **2022**, *56*, 102944. [[CrossRef](#)]
39. Ouyang, X.; Guo, Y.; Qiu, X. The feasibility of synthetic surfactant as an air entraining agent for the cement matrix. *Constr. Build. Mater.* **2008**, *22*, 1774–1779. [[CrossRef](#)]
40. *LVS 156-1:2022; Concrete*. National Annex to EN 206 Concrete. Specification, Performance, Production and Conformity. BSI: Englewood, CO, USA, 2022.